Supplement of Earth Syst. Sci. Data, 12, 1725–1743, 2020
https://doi.org/10.5194/essd-12-1725-2020-supplement

Open Access Earth System Science Data

Supplement of

A global monthly climatology of oceanic total dissolved inorganic carbon: a neural network approach

Daniel Broullón et al.

Correspondence to: Daniel Broullón (dbroullon@iim.csic.es)

Table S1. RMSE (bias) between measured and computed TCO_2 concentrations in several time series. Units are micromole per kilogram (µmol kg^{-1}). *There is only one sample below 500 m.

Depth range	BATS	HOT ALOHA	ESTOC	ICELAND	IRMINGER	K2	KNOT	OWS	KERFIX
0-50 m	8.7 (2.7)	5.8 (-2.6)	4.4 (-0.2)	7.8 (7.1)	5.3 (-0.1)	5.3 (0.3)	8.5 (-1.3)	10.1 (-5.3)	10 (23.9)
50-200 m	7.4 (-0.3)	6.2 (0.5)	7.7 (3.9)	4.8 (7.5)	4.9 (4.9)	3.6 (1.4)	5.4 (-0.9)	7.3 (-1.2)	10 (26.4)
200-500 m	6.1 (-1.8)	4.2 (0.9)	5.9 (1.9)	3.1 (6.2)	3.2 (5)	2.6 (1.2)	6 (-1.1)	3.9 (-1)	19.2 (28.8)
>500 m	6.4 (-2.7)	3.8 (-1.6)	6.6 (-0.6)	3.4 (3.3)	3.5 (5.5)	2.1 (1.7)	4.1 (-0.4)	3.1 (1.9)	-*

Table S2. Comparison between the TCO_2 climatology of Lauvset et al. (2016) and the one of the present study at different depth levels.

Depth layer	RMSE (µmol kg^{-1})	Bias (µmol kg^{-1})	r^2
0	31.5	-8.3	0.85
100	15.9	0.9	0.95
250	10.5	1.3	0.97
500	7.6	1.0	0.99
1000	6.8	0.4	0.99
2000	4.8	-0.4	0.995
3000	5.3	-1.4	0.993
4000	5.4	-1.2	0.99

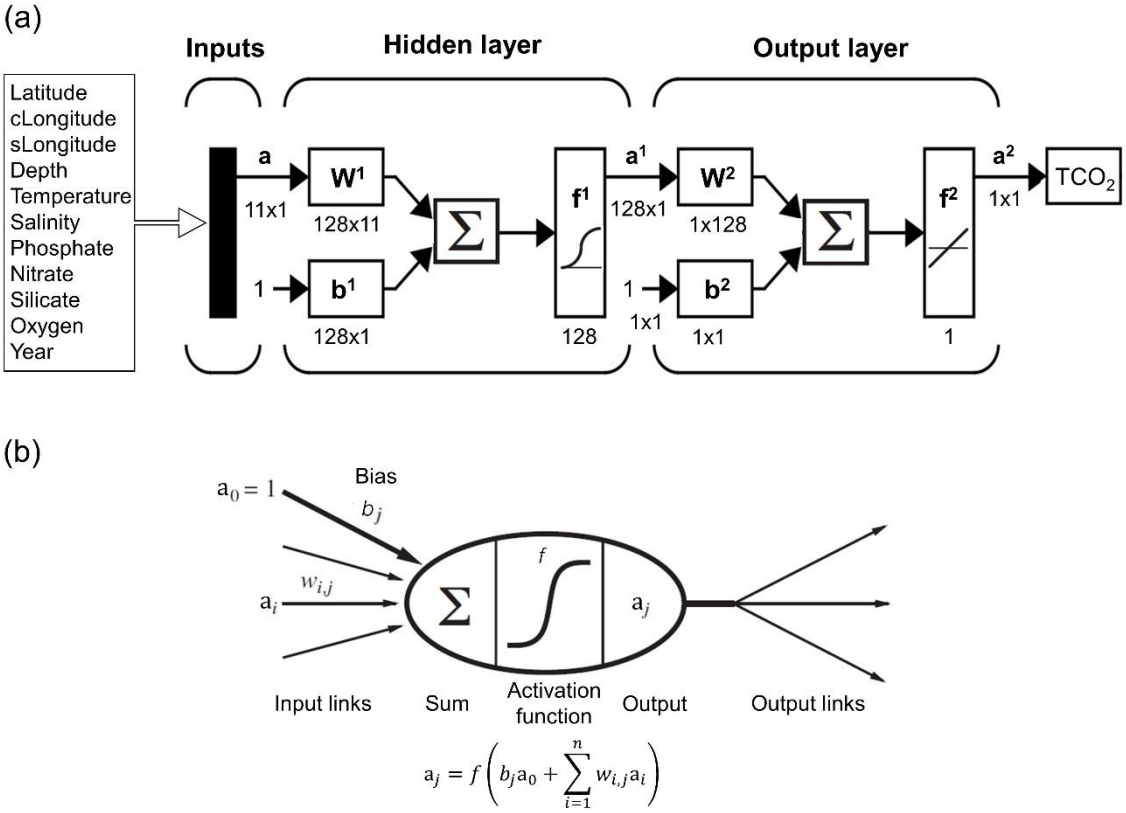

Figure S1. (a) Neural network configuration. The notation is in agreement with Hagan et al. (2014). **a**: input vectors; **W**: weight matrix; **b**: bias matrix; ∑: sum; f: transfer function; $\mathbf{a}^{\mathbf{X}}$: output matrix. The superscripts indicate the number of the layer. $cLongitude = cos(\frac{\pi}{180^{\circ}} longitude)$; $sLongitude = sin(\frac{\pi}{180^{\circ}} longitude)$. The dimensions of the matrices are for an individual sample. Modified from Hagan et al. (2014). (b) Neuron. a_i: inputs to each neuron; $w_{i,j}$: weights of each input to each neuron. Modified from Russell and Norvig et al. (2010).

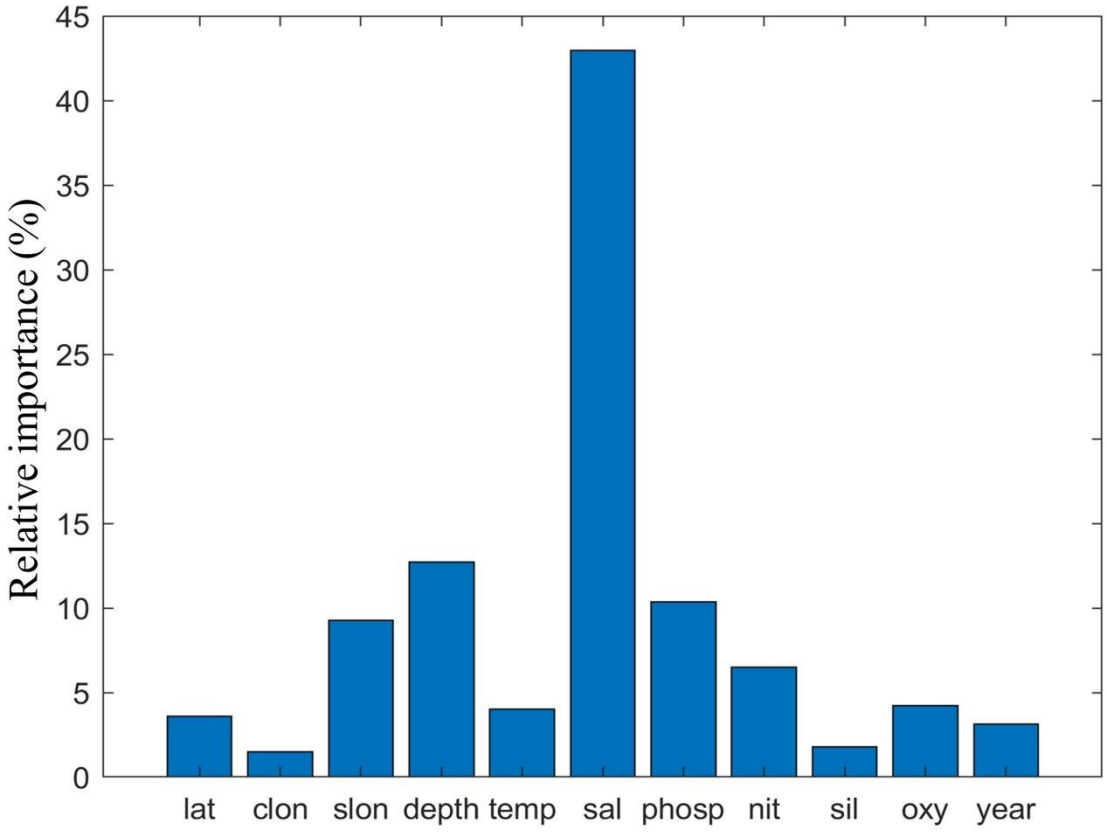

Figure S2. The relative importance of the input variables for NNGv2LDEO obtained with Eq. (1). lat: latitude; clon: clongitude; slon: slongitude; temp: temperature; sal: salinity; phosp: phosphate; nit: nitrate; sil: silicate; oxy: oxygen.

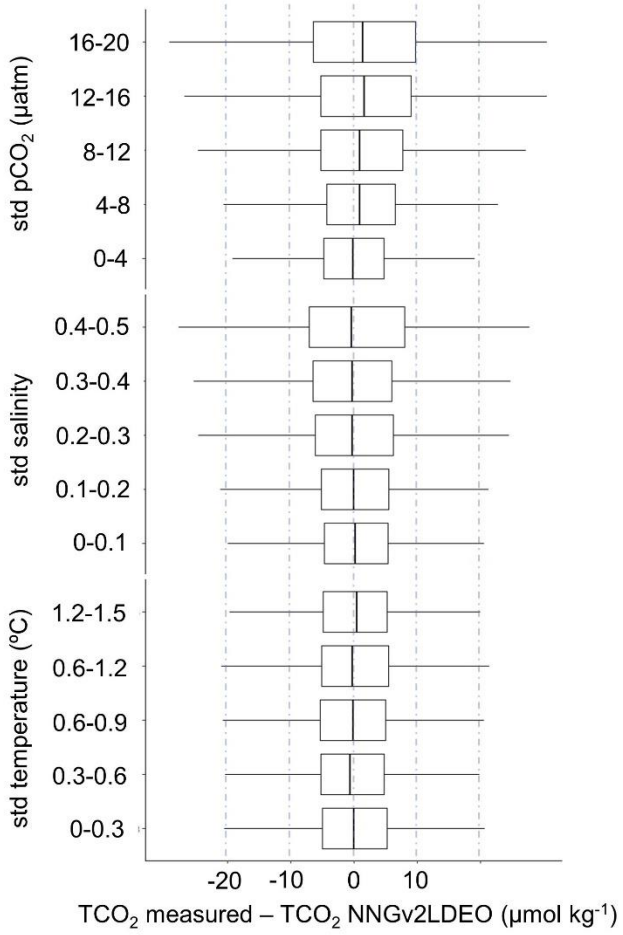

Figure S3. Box plots of differences between measured and computed TCO_2 in LDEO by standard deviation (SD) ranges obtained from the monthly average of the LDEO data.

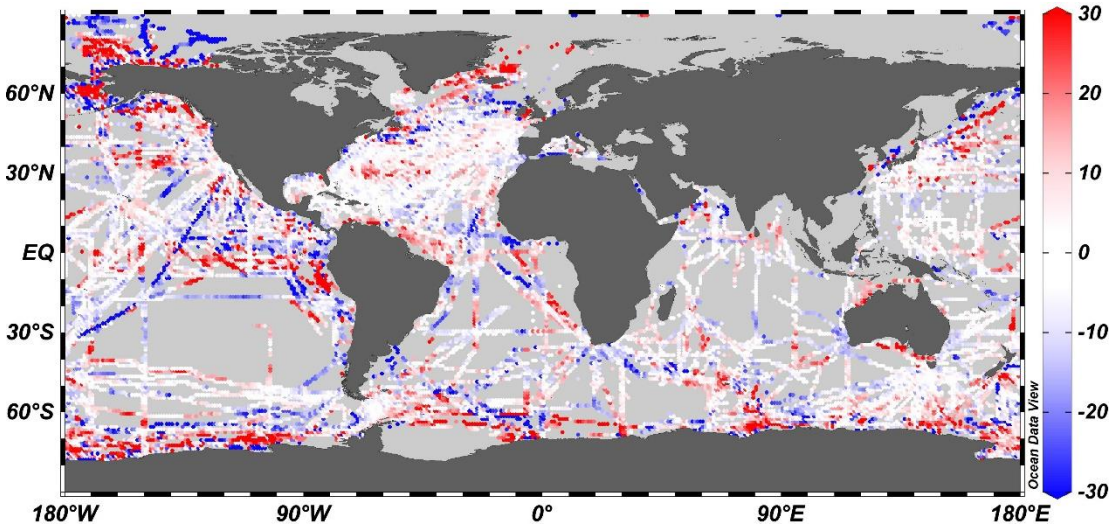

Figure S4. Differences between measured and computed pCO_2 with A_T from NNGv2 (Broullón et al., 2019) and TCO_2 from NNGv2LDEO in LDEO. Units are microatmospheres (µatm). This figure was made with Ocean Data View (Schlitzer, 2016).

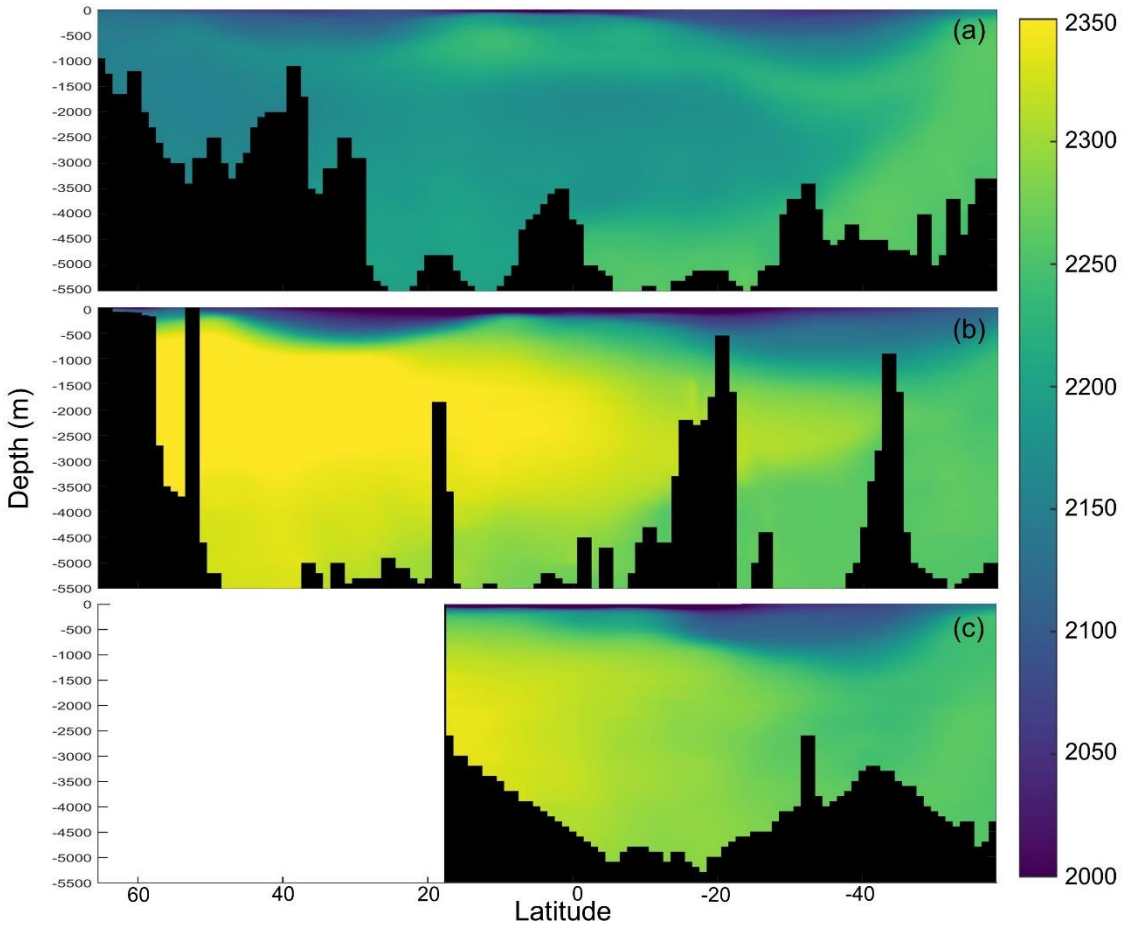

Figure S5. Sections of annual mean TCO_2 from the neural network climatology in (a) Atlantic (longitude: 28.5° W), (b) Pacific (longitude: 174.5° W) and (c) Indian (longitude: 84.5° E) oceans. Units are micromole per kilogram (µmol kg^{-1}).

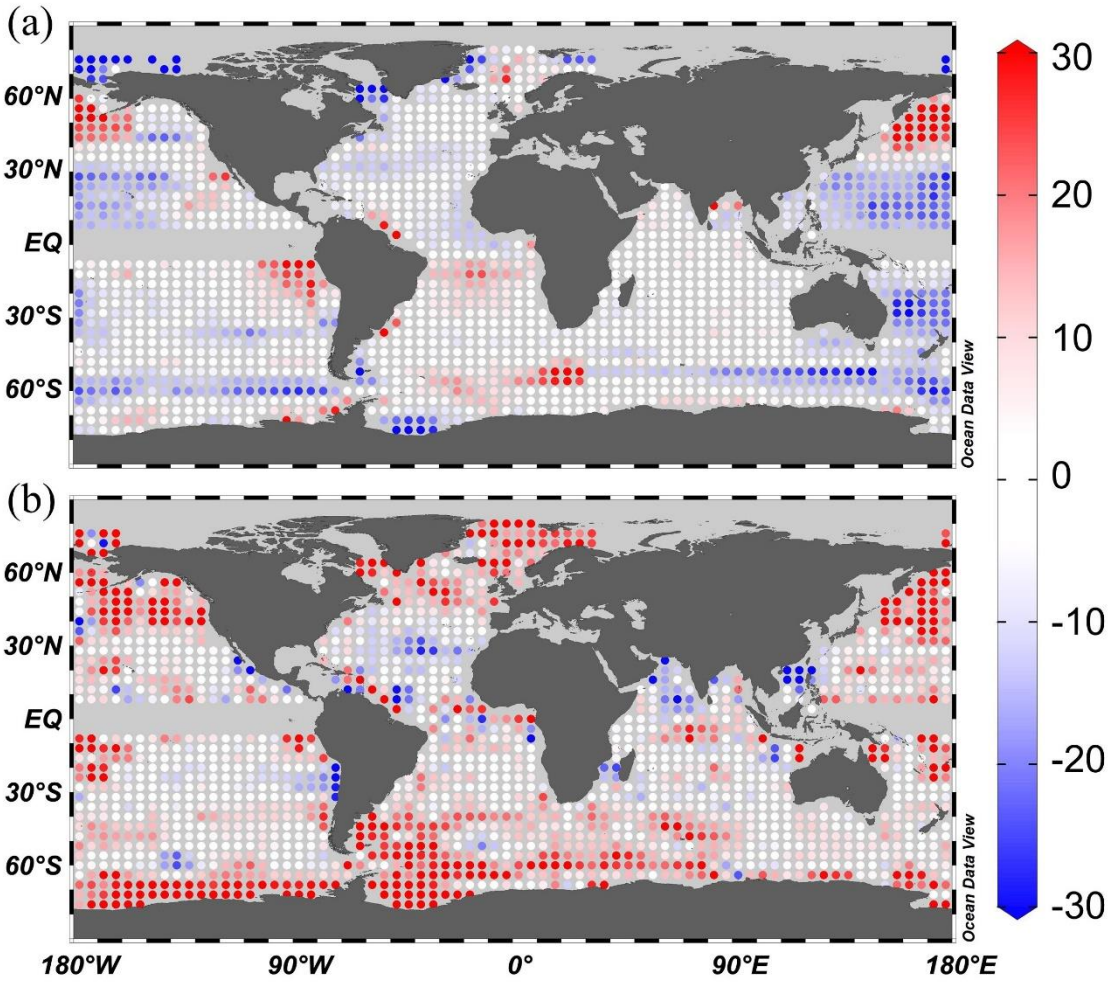

Figure S6. Differences between the annual mean of surface TCO_2 neural network climatology and (a) Takahashi et al. (2014) and (b) Lauvset et al. (2016) surface annual mean climatology. Units are micromole per kilogram (μmol kg^{-1}). The color bar was developed in order to show the highest differences beyond the errors of each method. This figure was made with Ocean Data View (Schlitzer, 2016).

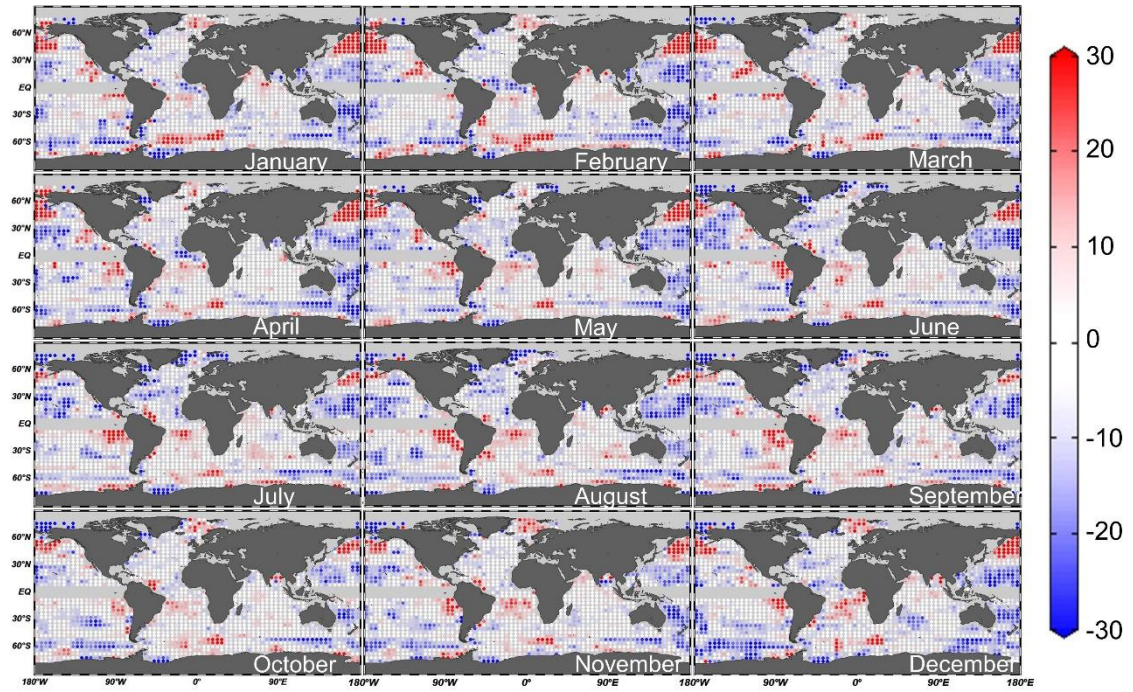

Figure S7. Differences between the monthly climatology of TCO_2 of Takahashi et al. (2014) and the one of the present study. The color bar was developed in order to show the highest differences beyond the errors of each method. Units are micromole per kilogram (μmol kg^{-1}). This figure was made with Ocean Data View (Schlitzer, 2016).

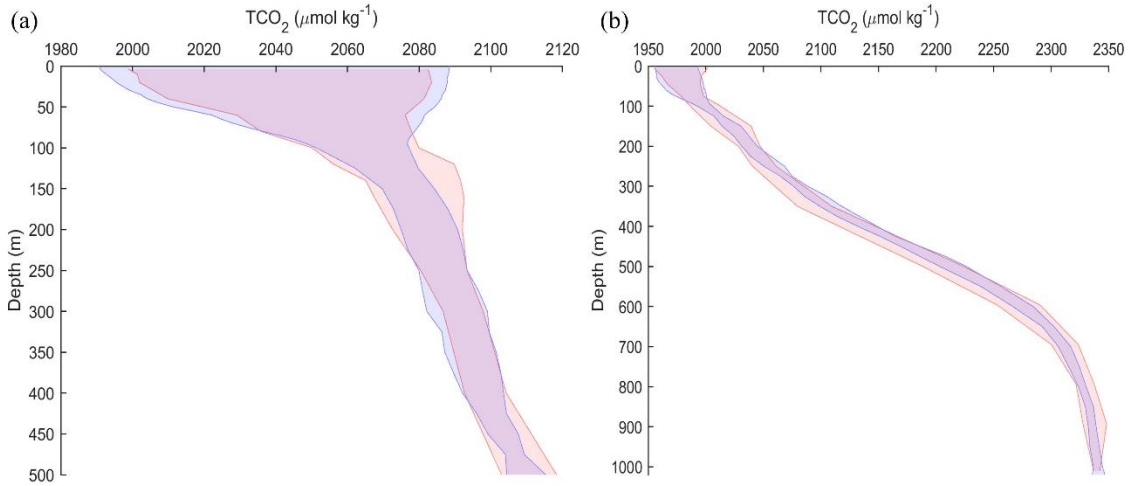

Figure S8. Profiles of the seasonal variability of the measured data (red lines and red shadow) and the TCO_2 climatology (blue lines and blue shadow) at (a) BATS and (b) HOT ALOHA locations. The variability of the measured data was computed subtracting the maximum and the minimum TCO_2 values of the measured climatological profiles depicted in Fig. 9. Note the different color of the overlapped area.

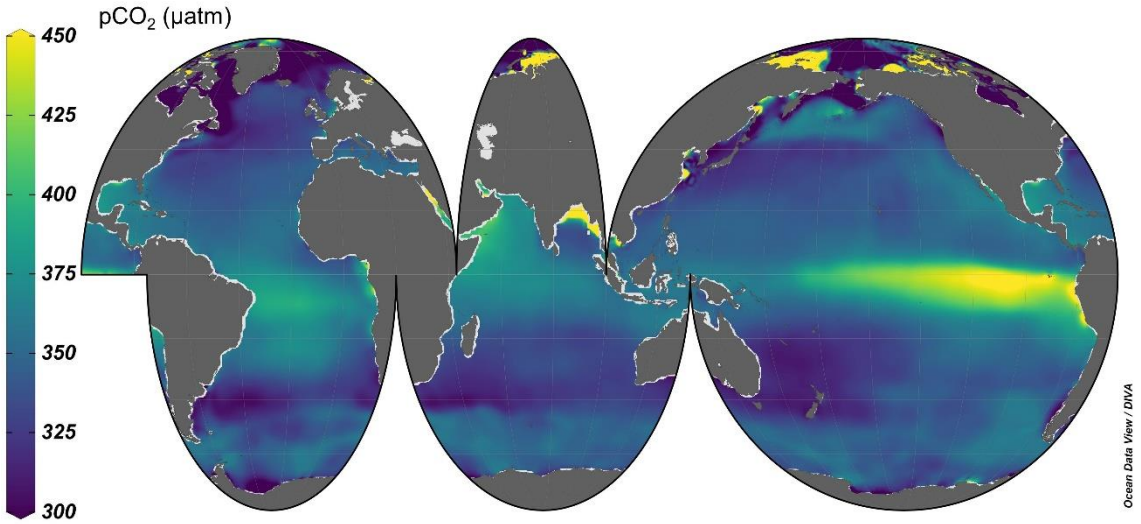

Figure S9. Annual mean pCO_2 centered in 1995 computed from the annual mean A_T (Broullón et al., 2019) and TCO_2 (this study). It should be noted that the extremely high values in the coastal waters of the Arctic Ocean are derived from a TCO_2/A_T ratio higher than 1. This fact is determined by the difficulty of neural networks to model both variables under the influence of river discharges with high concentrations of A_T and TCO_2, but TCO_2/A_T ratios higher than 1 are also found in the Arctic Ocean for the measured data in GLODAPv2.2019 (Olsen et al., 2019). This figure was made with Ocean Data View (Schlitzer, 2016).

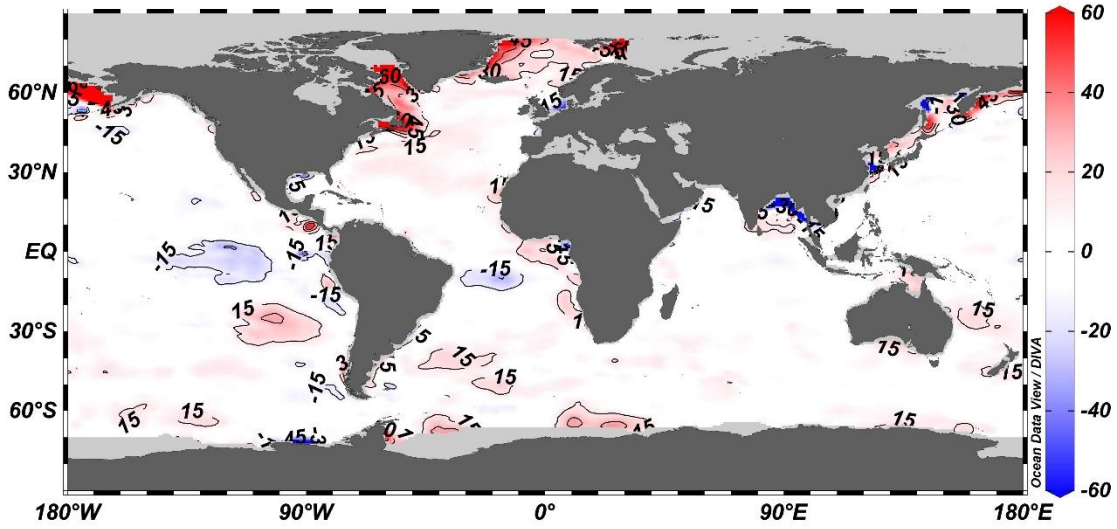

Figure S10. Differences between the annual mean climatology of pCO_2 from Landschützer et al. (2017) centered in 1995 and the one computed in the present study. Units are microatmospheres (µatm). The contour lines of 15, 30, 45 and 60 µatm are shown. This figure was made with Ocean Data View (Schlitzer, 2016).

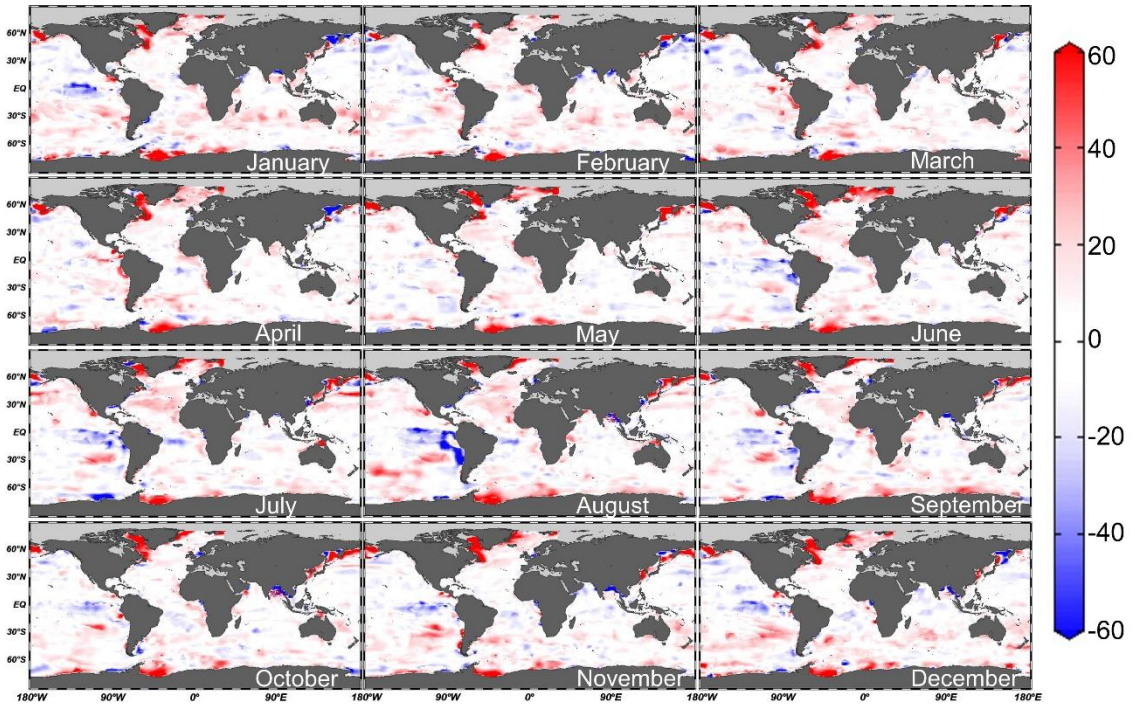

Figure S11. Differences between the monthly climatology of pCO_2 from Landschützer et al. (2017) centered in 1995 and the one computed in the present study. Units are microatmospheres (µatm). The contour lines of 15, 30, 45 and 60 µatm are shown. This figure was made with Ocean Data View (Schlitzer, 2016).

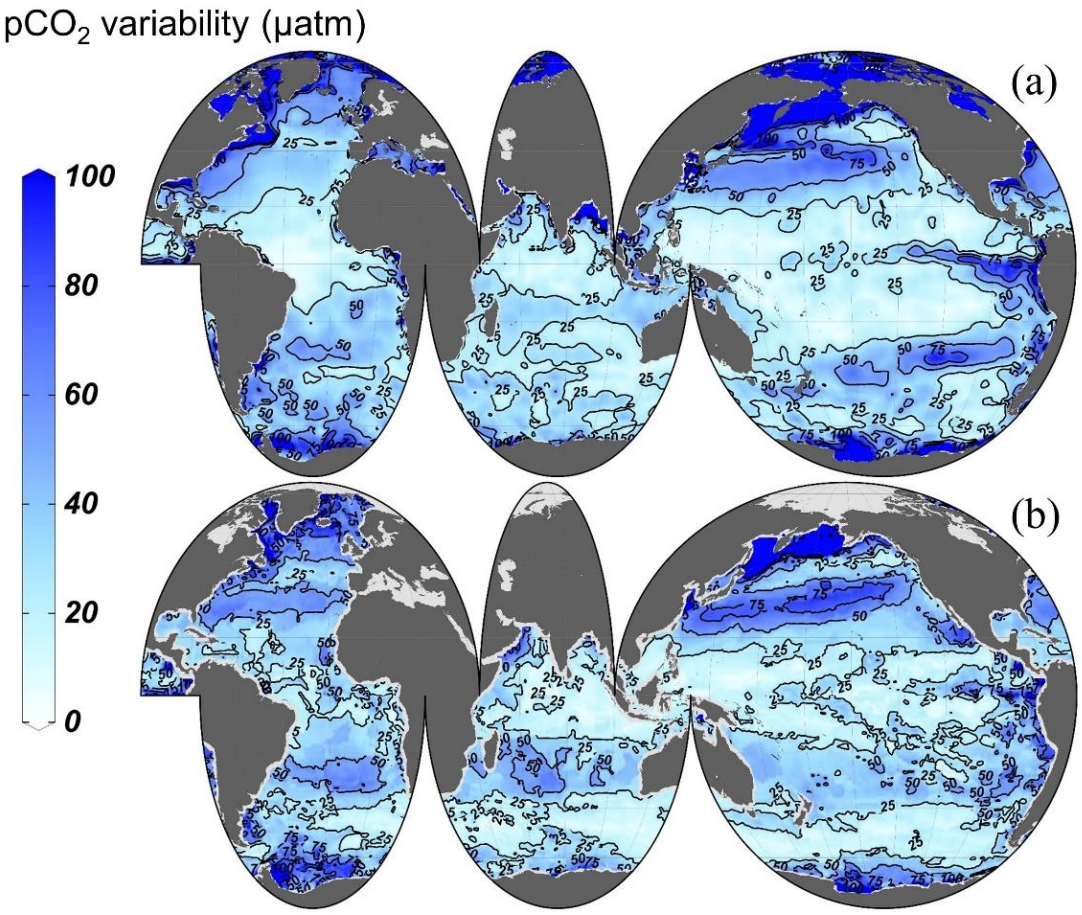

Figure S12. Seasonal amplitude of surface pCO_2 of (a) this study and (b) Landschützer et al. (2017) centered in the year 1995. The contour lines of 25, 50, 75 and 100 µatm are shown. This figure was made with Ocean Data View (Schlitzer, 2016).

References

Broullón, D., Pérez, F. F., Velo, A., Hoppema, M., Olsen, A., Takahashi, T., Key, R. M., Tanhua, T., González-Dávila, M., Jeansson, E., Kozyr, A. and van Heuven, S. M. A. C.: A global monthly climatology of total alkalinity: a neural network approach, Earth Syst. Sci. Data, 11(3), 1109–1127, doi:10.5194/essd-11-1109-2019, 2019.

Hagan, M. T., Demuth, H. B., Beale, M. H., and De Jesus, O.: Neural network design, ISBN 978-0971732117, available at: http://hagan.okstate.edu/nnd.html (last access: 26 July 2018), 2014.

Landschützer, P., Gruber, N. and Bakker, D.C.E.: An updated observation-based global monthly gridded sea surface pCO_2 and air-sea CO_2 flux product from 1982 through 2015 and its monthly climatology (NCEI Accession 0160558). Version 2.2. NOAA National Centers for Environmental Information. Dataset. [2017-07-11], (last access: 15 July 2019), 2017

Lauvset, S. K., Key, R. M., Olsen, A., Van Heuven, S., Velo, A., Lin, X., Schirnick, C., Kozyr, A., Tanhua, T., Hoppema, M., Jutterström, S., Steinfeldt, R., Jeansson, E., Ishii, M., Perez, F. F., Suzuki, T. and Watelet, S.: A new global interior ocean mapped climatology: The 1° × 1° GLODAP version 2, Earth Syst. Sci. Data, 8(2), 325–340, doi:10.5194/essd-8-325-2016, 2016.

Russell, S. J. and Norvig, P.: Artificial intelligence: a modern approach, Prentice Hall, 2010.

Schlitzer, R., Ocean Data View, available at: http://odv.awi.de (last access: 21 May 2018), 2016.